J Polym Res (2012) 19:9805
DOI 10.1007/s10965-011-9805-1

ORIGINAL PAPER

Electrical properties of multi walled carbon nanotubes/ poly(vinylidene fluoride/trifluoroethylene) nanocomposites

E. El Shafee · M. El Gamal · M. Isa

Received: 11 August 2011 / Accepted: 27 November 2011 / Published online: 22 December 2011

Abstract Poly(vinylidene fluoride-trifluoroethylene) (PVDF-TrFE)/multi-walled carbon nanotube (MWCNT) nanocomposites were prepared by the method of solution mixing/casting. The dispersity of the MWCNTs in the PVDF-TrFE matrix was investigated using transmission electron microscopy (TEM), revealing that MWCNT are well distributed in the PVDF matrix. Both individual and agglomerations of MWCNT's were evident. The electrical properties were characterized by ac conductivity measurements. The conductivity was found to obey a percolation-like power law with a percolation threshold below 0.30 wt. %. The electrical conductivity of the neat PVDF-TrFE could be enhanced by seven orders of magnitude, with the addition of only 0.3 wt. % MWCNTs, suggesting the formation of a well-conducting network by the MWCNT's throughout the insulating polymer matrix. The intercluster polarization and anomalous diffusion models were used to explain the dielectric behaviors of the composites near the percolation threshold, and the analyses of *ac* conductivity and dielectric constant imply that the intercluster polarization is more applicable to our systems.

Keywords Nanocomposites · Electrical conductivity · Percolation threshold · Poly(vinylidene fluoride-trifluoroethylene)

This paper was supported by Science and Technology Center, Cairo.

E. El Shafee (✉)
Chemistry Department, Faculty of Science, Cairo University,
12613 Giza, Egypt
e-mail: ezeldain@gmail.com

M. El Gamal · M. Isa
Science and Technology Center,
3 Cairo-Belbes Rd,
Cairo, Egypt

Introduction

Carbon nanotubes (CNT) have been the focus of extensive research efforts in the context of multifunctional composite materials [1, 2]. The discovery of electrically conductive behavior dominated by percolation at low filler loadings [3] has led to wide interest in the interplay between the processing and the electrical response of carbon nanotube based nanocomposites. Many polymer composites with CNTs have been obtained to date [1, 4–10]. Conductive polymer/CNT composites can be obtained at extremely low filler contents because of a large CNT aspect ratio (even >1000). A wide range of values of percolation thresholds and conductivities of CNT composites has been reported, depending on the processing method, polymer matrix, and the CNT type. However, a comparison of the literature data is difficult, and contradictory results can be found because various kinds of CNTs and different preparation methods have been used by different authors. As Bauhofer and Kovacs point out in their review [11], with optimized dispersion a percolation threshold in the range of 0.1 wt. % might be possible for nearly any CNT/polymer system.

Ferroelectric polymers such as poly(vinylidene fluoride) (PVDF) and its copolymers are important engineering polymers and have been extensively studied because of its excellent mechanical properties, resistance to chemicals, high dielectric permittivity and unique pyroelectric/piezoelectric properties [12, 13]. Because of these remarkable properties it is used to prepare conducting composites for self regulated heaters, over-current protectors, antistatic shielding, conducting electrodes for lithium batteries, and for other electrical applications [14].

Nanocomposites based on PVDF and CNTs have already been investigated. Levi and co-workers [15] were some of the first to study this system. They prepared nanocomposites

using single- and multi-walled carbon nanotubes (MWCNTs) with pure PVDF and its copolymers using the solution-casting method. The nanocomposites were found to exhibit enhanced pyroelectric and piezoelectric behavior over pure materials. Li et al. studied the electrical condutivity and dielectric properties of poly(vinylidene fluoride) (PVDF) composites filled with pristine, carboxyl and ester functionalized multiwalled carbon nanotubes (MWCNTs) [16]. A large dielectric constant of 3600 can be obtained in the carboxyl functionalized MWCNT/PVDF composite filled with 8 vol% MWCNT at 1 kHz. Almasri et al. [17] investigated the microstructure, electrical and thermomechanical behaviors of solution cast PVDF composites reinforced with double-walled CNTs. Their electrical measurement revealed that the PVDF/CNT nanocomposites exhibit a low percolation threshold (0.23 vol. %). PVDF/MWCNT nanocomposites prepared by melt blending were also studied [18, 19]. The percolation level in electrical conductivity was found to occur between 2 and 2.5 wt. %.

Copolymers, such as poly(vinylidene fluoride-co-trifluoroethylene) (P(VDF-TrFE)) and poly(vinylidene fluoride-trifluoroethylene-chlorofluoroethylene) (P(VDF-TrFE-CFE)) are also well known for their ferro-, piezo-, and pyeroelectric properties. They have great potential for applications in micro-electromechanical devices and high-charge storage capacitors [20–22]. In order to realize these applications, it was proposed to mix these copolymers with CNTs. Very few studies investigated the influence of CNT's content on the electrical properties of copolymer nanocomposites. For example Ramaratnam et al. [23] investigated the electrochemical response of piezoelectric CNT/P(VDF–TrFE) nanocomposites at 0.5% per weight ratio. They demonstrated an increase in the sensing capability of piezoelectric polymer composites by the addition of both SWCNTs and MWCNTs. For the CNT/P(VDF-TrFE-CFE) system the dielectric constant was found to increased from 57 to 102 (tan δ~0.36) at 100 Hz, by inclusion of only 2 wt% CNTs [24].

Here, we present a detailed study of the influence of MWCNT on the electrical conductivity of MWCNT/ P (VDF-TrFE) composites prepared using the common methods of solution mixing/casting. The electrical conductivities and the dielectric constant of these composites were investigated as a function of MWCNT's content. The electrical behavior of the composites near the percolation threshold were analyzed using two established theories, namely, the intercluster polarization and anomalous diffusion models, as shortly discussed in section 2.

Background

Electrical conductivity has been the most intensively studied property of composites near percolation since the physics of percolation was first introduced. When fillers with high electrical conductivity, σ_2, are continuously added to a matrix with low electrical conductivity σ_1, an abrupt increase in the electrical conductivity of their composites can be observed when the weight fraction P of the fillers approaches the critical weight fraction at percolation threshold P_c. This is especially so when the difference between the electrical conductivities of these two phases is large. These systems are usually modeled by a lattice, constructed of bonds chosen randomly to be a conductor or an insulator [25, 26].

According to the percolation theory, on the conducting side in the vicinity of the percolation threshold, a universal relationship between the electrical conductivity and the content of the conductive filler can be described as follows [27]:

$$\sigma_{dc}(p) \propto [p - p_c]^t \text{ for } P > P_c \quad (1)$$

where σ_{dc} is the electrical conductivity of the composite and t is the critical exponent primarily dependent on the topological dimensionality of the percolating system and not on the details of the structures or the interactions. On the other hand, on the insulating side of the percolation threshold, the σ_{dc} of a percolating system exhibits a power-law dependence on P_c - P as follows [28]:

$$\sigma_{dc}(p) \propto [p_c - p]^{-s} \text{ for } P < P_c \quad (2)$$

where s is the critical exponent.

The dependence of the real part of the permittivity, ε' on filler content near the percolation threshold P_c is given by [29]:

$$\varepsilon'(\mathrm{p}) \propto |\mathrm{P} - \mathrm{P_c}|^{-\mathrm{s}} \quad (3)$$

for both $P>P_c$ and $P<P_c$. According to Eq. (3), the dielectric permittivity is expected to diverge at the percolation threshold. The dielectric exponent s in Eq. (3) is also assumed to be equal to the exponent s, describing the divergent behavior of the *ac* conductivity (Eq.2).

Near the percolation threshold ($P \sim P_c$), both *ac* conductivity, σ_{ac} (ω,P_c), and the dielectric constant, ε' (ω,P_c), exhibit a kind of frequency dependence, varying as a power of ω, if they obey scaling forms that have singularities. The power-law behaviors are described as follows [29]:

$$\sigma_{ac}(\omega, p_c) \propto \omega^x \quad (4)$$

$$\varepsilon''(\omega, \mathrm{p_c}) \propto \omega^{-\mathrm{y}} \quad (5)$$

The critical exponents x and y are satisfied the following relationship: $x+y=1$.

Two classes of models have been developed for the description of the frequency dependence of the complex conductivity in percolating systems: (i) the 'equivalent circuit model', which treats a percolation system as a random mixture of resistors and capacitors (alternatively: resistors–isolators, resistors–superconductors, conductor–insulator, etc.) [30–32] and (ii) models based on charge carrier diffusion on percolation clusters [33].

Considering only the equivalent circuit model, a relationship was derived as follows [28–30, 34]:

$$x = \frac{t}{t+s} \quad \text{and} \quad y = \frac{s}{t+s} \tag{6}$$

However, the model of anomalous diffusion gives another relationship [33]:

$$x = \frac{t}{\nu(t+\theta)} \quad \text{and} \quad y = \frac{(2\nu-\beta)}{\nu(t+\theta)} \tag{7}$$

where ν, β and θ are the critical exponents dependent primarily on the dimensionality of the percolating systems, θ is given by $\theta=(t - \beta)/\nu$. Note that both Eqs. (6) and (7) satisfy the general scaling relation $x+y=1$.

In the present work the *ac* conductivity and dielectric spectra are discussed in terms of charge carrier diffusion on percolation clusters and resistor–capacitor composites.

Experimental

Materials

Non functionalized MWCNT's were used and was supplied by Nanostructured & Amorphous Materials, Inc. USA, with a purity of > 95%, nominal outside diameter and length of 40–50 nm and 5–15 μm, respectively. The matrix used for the preparation of nanocomposites is a random copolymer of P(VDF–TrFE) (Piezotech in France), TrFE content of 30 wt. %. Methy ethyl keton (MEK) as a solvent was obtained from Aldrich and used without further purifications.

Preparation of nanocomposites

The nanocomposites were prepared by solution mixing/casting. The MWCNT's were ultrasonically dispersed in methyl-ethyl-ketone (MEK) at the room temperature for 2 h to form a stable suspension. In order to not break the nanotubes two precautions were taken. One was to set the probe to work with only 50% of maximum amplitude and the second one was to set it to work in pulses. At the same time, the P(VDF-TrFE) copolymer was also dissolved in MEK. Then the suspension of MWCNT's in MEK was added to the PVDF-TrFE solution, the mixture was magnetic stirred for 30 min, then subjected to ultrasonic treatment for another 30 min.

The MWCNT concentration needed in the solvent was calculated in order to obtain a loading of 0.05 to 0.8 wt. % in the final composite. The final nanocomposite solutions were cast in 50 ml petri-dish, degassed in a vacuum oven, and kept in hood for a period of 48 h for the solvent evaporation. The films were dried at room temperature, peeled off from the petri-dish and annealed at 120 °C for 12 h. The groups of films fabricated in this way have a thickness of 0.4–0.6 mm.

Measurements

The alternating current electrical properties of the nanocomposites were measures using BDS 1200 cell connected to impedance Analyzer Hewlett–Packard 4284 for frequencies from 20 Hz to 1 *M*Hz. Prior to the measurement, the samples are electroded using a silver paint to create a thin conductive sheet on either side of the sample to act as a parallel plate electrode (area~1 cm^2). The morphology of the samples was examined by transmission electron microscopy (TEM). For TEM measurements, ultra thin sections were prepared with an Ultracut E ultramicrotome by Reichert and Jung using a diamond knife. Measurements were carried out on a high resolution Ticnai G20 microscop (200 kV).

Results and discussion

Observation of CNT network

The distribution and dispersion of CNT within the polymer matrix were examined by TEM. Figure 1 shows TEM micrographs of composite containing 0.15 wt. % and 0.30 wt.% of carbon nanotubes. The TEM observation reveals a homogenous dispersion of CNTs in P(VDF–TrFE) matrix, and CNTs are randomly dispersed without preferred alignment. With a high magnification, individual CNTs can be clearly viewed in the different regions (see Fig. 2). The CNTs remain curved or even interwoven throughout P (VDF–TrFE) matrix, indicating their extreme flexibility. Most of CNTs embedded into the matrix show some degree of waviness or entanglements along axial direction. These results are consistent with those reported by Liu [35]. Although TEM can clearly visualize the individual nanotubes, it is difficult to draw a conclusion concerning the global dispersion of CNTs in the nanocomposites. Both individual and agglomerations of MWCNT's were evident at all compositions.

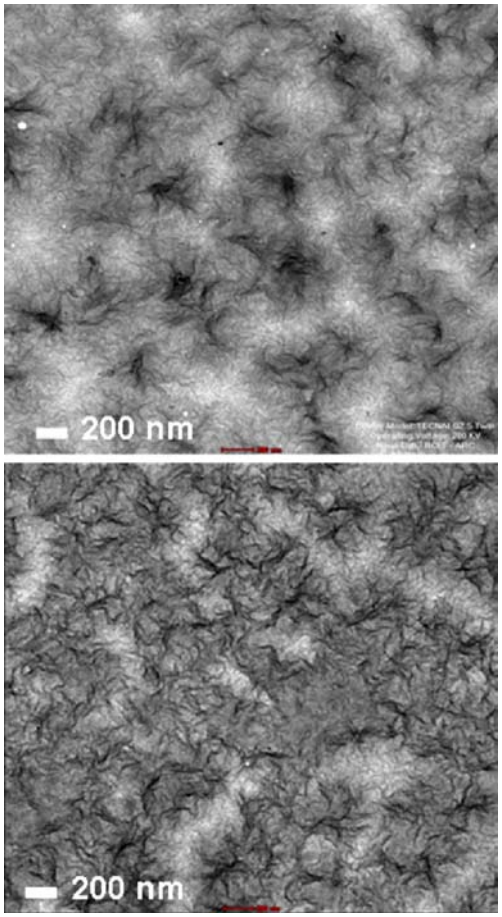

Fig. 1 TEM micrographs of P(VDF–TrFE)-based nanocomposites with different CNT volume contents: **a** 0.15 wt.%, **b** 0.3 wt.%

Conductivity and dielectric spectra

Figure 3 shows the frequency (*f*) dependence of the *ac* conductivity of the CNT/ PVDF-TrFE with various CNT weight contents measured at room temperature. For pure PVDF-TrFE, the *ac* conductivity increases linearly with increasing frequency, exhibiting a typical capacitor behavior (i.e. as a dielectric) where the conductivity follows the equation

$$\sigma_{ac} = 2\pi f \varepsilon_o \varepsilon'' \quad (8)$$

where ε'' is imaginary part of the complex permittivity and ε_o is the vacuum permittivity.

For the CNT/PVDF-TrFE composites, the change in *ac* conductivity with frequency provides information about the overall connectivity of the conducting network and can be categorized into three behaviors according to the size and distribution of the conductive clusters. Below the percolation threshold (for P=0.1), the *ac* conductivity increases continuously with frequency as $f^{\sim 0.8}$ (for f>500 Hz). This behavior is characteristic of finite size clusters displaying a broad distribution of sizes [36]. It is also consistent with the model of tunnel conductivity between finite size clusters developed by Sarychev and Brouers [37]. Just above the percolation threshold (P=0.3), an infinite cluster spans the whole system: the *ac* conductivity remains constant and equal to the *dc* up to a characteristic frequency (f_c) above which diffusion of carriers is limited to lengths that are equal to site or smaller than that of the finite size clusters [38] and of dangling ends. At larger volume fractions, the mean size of the finite clusters decreases in such a way that f_c becomes larger than the upper limit of the frequency domain investigated here. It follows that σ_{ac} remains constant and equal to σ_{dc} over the whole range of frequency investigated.

Plots of *ac*-conductivity vs. frequency especially at lower frequency (σ_{ac} vs. f) for all systems were extrapolated to

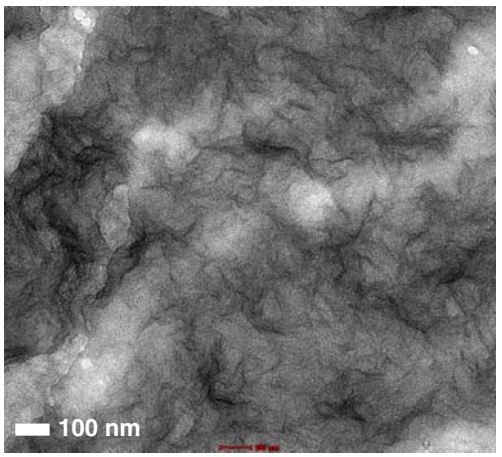

Fig. 2 TEM-images of a curved and entangled nanotubes in a 0.15 wt.% CNT filled P(VDF–TrFE) composite

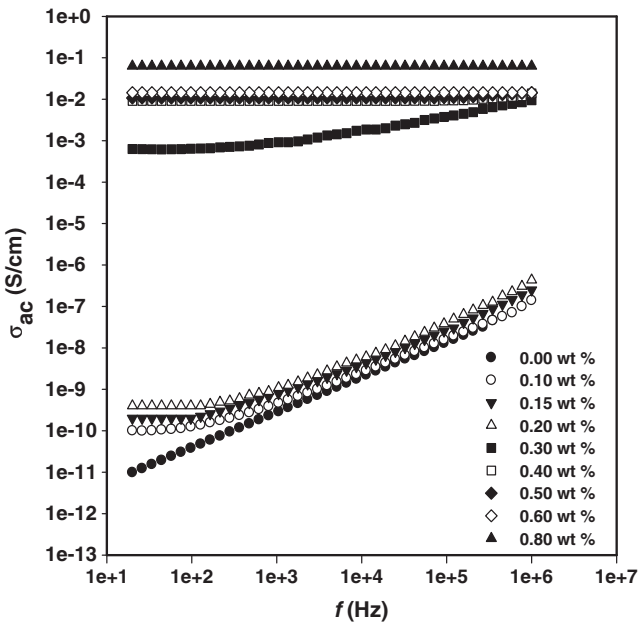

Fig. 3 Variation of the ac conductivity with frequency,f, for different MWCNT weight fractions, at room temperature

zero frequency. The electrical conductivity observed at zero frequency for each system was considered as *dc*-conductivity, σ_{dc} (according to the Eq. $\sigma'(\omega) = \sigma_{dc} + \sigma_{ac}(\omega) = \sigma_{dc} + A\omega^s$). These values for σ_{dc} were used as experimental *dc*-conductivities to check the percolation limit for different composites. Figure 4 represents the extrapolated values of the σ_{dc} data as a function of CNT weight fraction for the nanocomposites. As can be seen, there is an increase in conductivity of about seven orders of magnitude when increasing the loading fraction from 0.2 to 0.3 wt%. A further increase in nanocomposite conductivity to values above 0.001 S/cm appears for loading fractions of more than 0.3 vol%. At higher CNT loadings, e.g., between 0.6 and 0.8 wt%, the conductivity stabilizes at around 0.05 S/cm, which is, to the best of our knowledge, the highest value ever reported for CNT/thermoplastic nanocomposites at this low level of CNT loading. Comparable conductivity levels have been reported for CNT loadings far exceeding 1.0 wt% (see reference [11] and articles cited therein).

Figure 5 presents the room temperature dielectric permittivity (ε') versus frequency (f) for the samples which exhibit insulating behavior. The concentrations above P_c (0.3 wt% CNT) are also included in order to show the difference which is observed at P_c. As can be seen, when $P<P_c$, the dielectric constant decreases very slowly with the increase of frequency; when $P \geq P_c$, the dielectric constant reduces sharply in the low-frequency range, followed by a gradual decrease in the high-frequency range. The significant increment in dielectric constant of CNT/P(VDF-TrFE) nanocomposites can be mainly attributed to the homogenous dispersion of CN in the PVDF-TrFE polymer matrix and a gradual formation of the microcapacitor networks in the CNT/(PVDF-TrFE) nanocomposites as the CN content increases. Figure 6 shows the evolution of the dielectric constant at 1 kHz in the CNT/(PVDF-TrFE) nanocomposites with the change of CN content. As shown in Fig. 6, when a small amount of CN s is incorporated into the PVDF-TrFE matrix, some microcapacitance structures are formed, resulting in a slight increase of dielectric constant relative to that of pure P(VDF-TrFE). As the CN content is further increased, the dielectric constant gradually rises. Up to the percolation threshold, there are many CNs agglomerates isolated by very thin dielectric insulating-polymer layers within the nanocomposites, forming lots of microcapacitors, which leads to a very high dielectric constant. Then, beyond the percolation threshold, the dielectric constant of the CNT/PVDF-TrFE keeps on rising, because the CN are still wrapped by a thin layer of polymer matrix, if they are well dispersed. In addition, owing to the Maxwell–Wagner–Sillars (MWS) polarization a lot of charges were blocked at the interfaces between the filler and polymer matrix and makes a remarkable contribution to the increment of the dielectric constant in the low-frequency range.

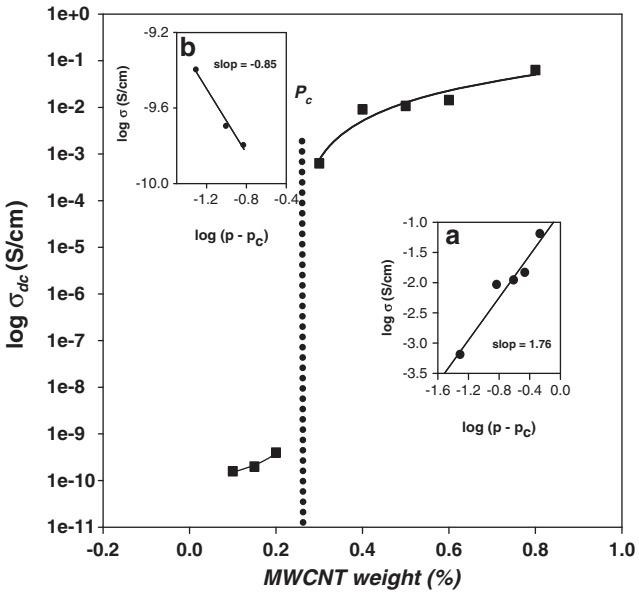

Fig. 4 Main figure, composite conductivity, σ_{dc}, plotted against MWCNT wt. %. Inset **a**, log σ_{dc} plotted against log (P–P_c) for $P>P_c$. Inset **b**, log σ_{dc} plotted against log (P–P_c) for $P<P_c$. P_c is the critical weight fraction at percolation threshold (see text)

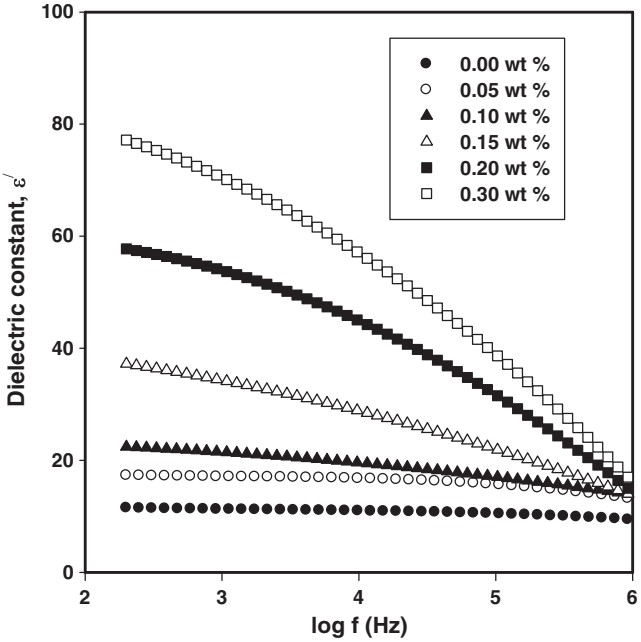

Fig. 5 Dielectric constant versus frequency with different wt % MWCNT measured at room temperature

In order to get an estimate for P_c and the critical exponents t and s; we fitted first the σ_{dc} data for $P>P_c$ to Eq. (1). This was done by variation of P_c in the interval from 0.2 to 0.3 in steps of 0. 01. For each value of P_c, the value of t has been determined from the slope of the linear relation of σ_{dc} and P–P_c on a log–log scale, as seen in insert (a) of Fig. 4. The lowest value of the root mean square error was found for P_c= 0.24 with the exponent t=1.76. Then, the σ_{dc} data for $P<P_c$

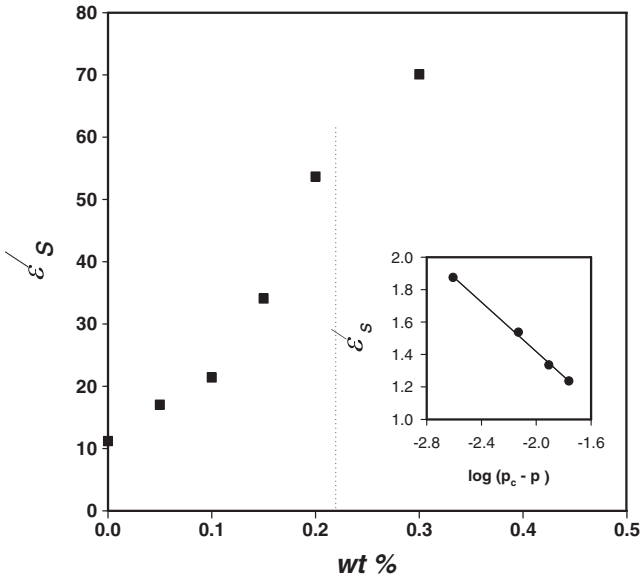

Fig. 6 Dielectric constant at 1 kHz as a function of MWCNT wieght fraction

was fitted to Eq. (2) with P_c=0.24 (obtained above) to estimate the critical exponent *s*. The best fit to the data is shown in insert (b) of Fig. 4 and gives s=0.84.

Typical values of t reported for CNT-polymer composites are in the range of 1.3–4, see [11], although a few works report values of t of~4.9 [39] and even higher than 7 [40]. Mathematically, since P–P_c is a small fraction (<1), a lower value of t in Eq. (1) means more abrupt increments in electrical conductivity in the vicinity of percolation (7 orders of magnitude in our case). The physical interpretations of the critical exponent t is more complex, and still a matter of controversy, as stated in a recent review by Bauhofer and Kovacs [11]. This exponent is frequently associated to the system dimensionality, with values of t≈1.3 (or slightly higher) representing a two-dimensional network and t≈2 (or slightly higher) a three dimensional one [39].

The low conductivity exponent t (=1.76 in our case) does not reflect a reduction in system dimensionality in the present case but rather the aggregation process of the carbon nanotubes during sample preparation. In other words, the formation of these conducting networks is not a true statistical percolation process based on the random distribution of individual high aspect ratio fillers, but rather is attributed to the mutual attraction of the nanotubes. This would mean that the percolation takes place in a network displaying a large number of dead arms and the network deviates from a classical random network [5].

On a similar way the variation of dielectric constant near the percolation threshold was fitted to Eq. 3. The best linear fit for ε' vs. (P - P_c) data on a log–log scale is presented in Fig. 6. The critical exponent s is 0.76. The percolation exponent obtained is very near to the theoretical value of ν=0.73 for percolation network formed by a random mixture of complex resistors [28]. It is worth mentioning that according to Eq. (3), the dielectric constant is expected to diverge at the percolation threshold. However, it is seen that the dielectric constant of the composites remains increase above the percolation threshold (see Fig. 6) but does not decrease as expected from Eq. 3. Such behavior has been reported earlier for polymer composites containing carbon black [41] and was attributed to "micro capacitors" remaining in the sample above the percolation threshold. The "micro capacitors" are assumed to be formed by gaps between multiwall carbon nanotubes.

Substituting t and s by the experimental data in Eq. (6), we can obtain x=0.7 and y=0.30. On the other hand, using the established value for θ, ν, and β (in diffusion model, θ~ 1.5, ν~0.9 and 2ν - β=1.3) [33], the estimated value via Eq. (7) gives x=0.58 and y=0.42. Our experimental results give the value of x=0.78±0.05 and y=− 0.11±0.04, which are closer to the calculated results based on the intercluster polarization model than those from the anomalous diffusion model, so the intercluster polarization theory is more applicable for the present percolating systems in the frequency range of measurement. The discrepancy between the experimental data and the anomalous diffusion theory is considered to be relevant with the fact that this model takes no account of the phonon-assisted tunneling through barriers separating the CNT clusters and other transport effects, such as trapping and hopping, between the clusters [42].

Comparison between the experimental and the theoretical P_c

At that point, it is interesting to compare the experimentally calculated value of P_c to the theoretical one. Simple theoretical models using continuum percolation and considering the filler network as a group of non-interacting sticks of high aspect ratio, give an order of magnitude of the percolation threshold value (in volume fraction), which scales as $1/\eta$ (where η is the aspect ratio of the MWCNT), by considering that the rod number density is roughly the reciprocal of the excluded volume of the rods [43, 44]. For the systems considered here, the values of the percolation thresholds are expected to be of the order of ~0.0045 wt. % (by considering a length of ~10 μm and a diameter of 45 nm per specification of the MWCNT used. The density of MWCNT is ~1.8, and that of the copolymer is ~1.78).

However, the experimental value of percolation threshold measured (see Fig. 4) is about fifty times higher than the predicted ones. In fact, as CNTs in polymer composites appear curved or wavy and entangled (see Fig. 2), this will lead to an underestimation of the percolation threshold by the excluded volume approach because the effective length of curved tubes is shorter than that for a straight rods [45]. The effect of waviness on percolation has been investigated by Berhan et al. [46]. Their calculations show that waviness

of CNTs alone, assuming ideal dispersion, leads to an increase of percolation threshold of up to a factor of two, which means that the effect of waviness can be considered as small. Consequently, other factors must contribute to such a high percolation threshold.

It is known that for a semicrystalline polymer such as P (VDF-TrFE), there is phase separation between crystalline and amorphous regions, and MWCNTs were found to be confined in the amorphous region [47] (one of the main causes of MWCNT aggregation). Thus phase separation might have negative effects on the dispersion of MWCNTs inside the matrix. Further, the presence of a thin polymer layer can prevent direct contact between CNTs [48], and this can increase the effective percolation threshold by reducing the number of CNT-CNT contacts which are electrically conducting [49].

Conclusions

The electrical properties of the solution prepared MWCNT/ P (VDF-TrFE) nanocomposites were investigated. Solution mixing enabled homogeneous dispersion of MWCNT's within P(VDF-TrFE) matrix, as revealed by TEM. The results showed that the electrical behavior of MWCNT/ P(VDF-TrFE) nanocomposites can be well described by the percolation theory. Both conductivity and dielectric constant were found to be greatly enhanced in the vicinity of percolation threshold. The electrical conductivity of the neat PVDF-TrFE could be enhanced by seven orders of magnitude, with the addition of only 0.3 wt. % MWCNTs, suggesting the formation of a well-conducting network by the MWCNT's throughout the insulating polymer matrix. The conductivity of the composite film near the percolation threshold is ~10^{-3} S cm^{-1}. This can be a beneficial feature for, e.g., macroscale strain sensor applications because of the relative ease of detecting conductivity change near the percolation threshold induced by strain [50]. Two established theories were used to investigate the behaviors of the composites near the percolation threshold, and then the results indicated that the intercluster polarization effect is more reasonable to explain the electrical property of our system in the frequency range of measurement.

References

1. Moniruzzaman M, Winey KI (2006) Macromolecules 39:5194–5205
2. Thostenson ET, Li C, Chou TW (2005) Compos Sci Technol 65:491–516
3. Coleman JN, Curran S, Dalton AB, Davey AP, McCarthy B, Blau W, Barklie RC (1998) Physical Review B—Condensed Matter and Materials Physics 58(12):R7492–R7495
4. Thostenson ET, Ren Z, Chou T-W (2001) Compos Sci Technol 61:1899
5. Barrau S, Demont P, Peigney A, Laurent C, Lacabanne C (2003) Macromolecules 23:5187
6. Breuer O, Sundararaj U (2004) Polymer Compos 25:630–645
7. Khare R, Bose S (2005) Journal of minerals and Materials Characterization and Engineering 4:31–46
8. Zhang QH, Rastogi S, Chen DJ, Lippits DR, Lemstra PJ (2006) Carbon 44:778
9. Zhang QH, Lippits DR, Rastogi S (2006) Macromolecules 39:658
10. Mylraganam K, Zhang LC (2007) Recent Patent on Nanotechnology 1:59–65
11. Bauhofer W, Kovacs JZ (2009) Compos Sci Technol 69(10):1486–1498
12. Chen GX, Li YJ, Shimizu H (2007) Carbon 45:2334–2340
13. Fuan H, Jintu F, Sienting L (2008) PolymTest 27:964–970
14. Giannelis PE, Ansari S (2009) J Polym Sci B: Polym Phys 47:888–897
15. Levi N, Czerw R, Xing S, Iyer P, Carroll LD (2004) Nano Lett 4:1267–1271
16. Li Q, Xue Q, Hao L, Gao X, Zheng Q (2008) Compos Sci Technol 68:2290–2296
17. Almasri A, Ounaies Z, Kim YS, Grunlan J (2008) Macromol Mater Eng 293:123–131
18. Nam YW, Kim WN, Cho YH (2007) Macromol Symp 249–250:478–484
19. Hong SM, Hwang SS (2008) J Nanosci Nanotechnol 8:4860–4863
20. Zhang QM, Li HF, Poh M, Xu HS, Cheng ZY, Xia F, Huang C (2002) Nature 419:284
21. Zhang QM, Bharti V, Zhao X (1998) Science 280:2101
22. Naber CG, Tanase C, Blom PWM, Gelinck GH, Marsman AW, Touwslager FJ, Setayesh S, De Leeuw DM (2005) Nat Mater 4:205
23. Ramaratnam A, Jalili N (2006) Journal of Intelligent Material System and Structure 17:199–208
24. Zhang SH, Zhang NY, Huang C, Ren KL, Zhang QM (2005) Adv Mater 17:1897
25. Bunde A, Havlin S (1996) Fractals and disordered systems. Springer, Berlin
26. Sahimi M (1994) Applications of percolation theory. Taylor & Francis, London
27. Kirkpatrick S (1971) Phys Rev Lett 27(25):1722–1725
28. Webman I, Jortner J, Cohen MH (1977) Phys Rev B 16(6):2593–2596
29. Bergman DJ, Imry Y (1977) Phys Rev Lett 39(19):1222–1225
30. Efros AL, Shklovskii BI (1976) Phys Status Solidi B 76(2):475–485
31. Stroud D, Bergman DJ (1982) Phys Rev B 25(3):2061–2064
32. Wilkinson D, Langer JS, Sen PN (1983) Phys Rev B 28(2):1081–1087
33. Gefen Y, Aharony A, Alexander S (1983) Phys Rev Lett 50(1):77–80
34. Song Y, Noh TW, Lee SI, Gaines JR (1986) Phys Rev B 33(2):904–908
35. Liu TX, Phang IY, Shen L, Chow SY, Zhang WD (2004) Macromolecules 37:7214–7222
36. Benaboud K, Achour ME, Carmona F, Salome L (1998) Ann Chim Sci Mat 23:315–318
37. Sarychev AK, Brouers F (1994) Phys Rev Lett 73:2895–2898
38. Adriaanse LJ, Reedijk JA, Teunissen PA, Brom HB, Michels MAJ, Brokken-Zijp JMC (1997) Phys Rev Lett 78:1755–1758
39. Antonucci F, Faiella G, Giordano M, Nicolais L, Pepe G (2007) Macromol Symp 247:172–181
40. Ha MLP, Grady BP, Lolli G, Resasco DE, Ford TW (2007) Macromol Chem Phys 205:446–456
41. Flandin L, Prasse T, Schueler R, Schulte K, Bauhofer W, Cavaille JY (1999) Phys Rev B 59(22):14349–14355
42. Achour ME, Brosseau C (2008) J Appl Phys 103(9): 094103-1–094103-10.
43. Balberg I, Anderson CH, Alexander S, Wagner N (1984) Phys Rev B 30:3933–3943

44. Bug ALR, Safran SA, Webman I (1985) Phys Rev Lett 54:1412
45. Dalmas F, Dendievel R, Chazeau L, Cavaille JY, Gauthier C (2006) Acta Mater 54:2923
46. Berhan L, Sastry AM (2007) Phys Rev E 75(4):41121
47. Shieha YT, Liua GL, Hwangb KC, Chen CC (2005) Polymer 46:10945–10951
48. Balberg I, Azulay D, Toker D, Millo O (2004) Int J Mod Phys 18:2091
49. Bryning MB, Islam MF, Kikkawa JM, Yodth AC (2005) Adv Mater 17:1186
50. Park M, Kim H, Youngblood JP (2008) Nanotechnology 19: 055705